

Morphology evolution and phase transition of $\text{Co}(\text{OH})_2$ and Co_3O_4 investigated with STEM-tomography and in-situ XRD

Olivia Kaya Gerds^{1,2,3}, Lars Fahl Lundegaard³, Hanne Falsig³, Christian Danvand Damsgaard^{1,2,4}, Lars Pilsgaard Hansen³

¹Center for Visualizing Catalytic Processes (VISION), Department of Physics, Technical University of Denmark, Kgs. Lyngby, Denmark, ²Surface Physics and Catalysis, Department of Physics, Technical University of Denmark, Kgs. Lyngby, Denmark, ³Topsoe A/S, Kgs. Lyngby, Denmark, ⁴National Center for Nano Fabrication and Characterization, Technical University of Denmark, Kgs. Lyngby, Denmark

Background incl. aims

Transition metal hydroxides ($\text{TM}(\text{OH})_2$) have garnered significant attention in research due to their diverse applications in the energy and environmental sectors. These hydroxides exhibit promising capabilities in catalysis, supercapacitors, and battery materials [1-3]. For instance, cobalt hydroxides ($\text{Co}(\text{OH})_2$) can decompose to form cobalt oxides (e.g., Co_3O_4), which are materials known for their applications as catalysts in the Fisher-Tropsch process, water splitting, and N_2O decomposition [1,4].

Catalytic processes typically occur at elevated temperatures. Understanding the morphological changes and phase transitions of Co_3O_4 upon heating is crucial for controlling its properties in various applications, including those listed above. Furthermore, studies suggest that besides particle size and morphology, the distribution of exposed facets in Co_3O_4 plays a role in the catalyst's activity during N_2O decomposition [4].

In this work, a visualization of the morphological evolution of Co_3O_4 crystals synthesized by calcination of $\text{Co}(\text{OH})_2$ at different temperatures is carried out through ex-situ (S)TEM imaging of samples. Furthermore, the facet distribution of a Co_3O_4 particle, revealing the concentration of exposed surfaces, is determined and visualized in 3D by combining STEM-HAADF electron tomography (ET) and high-resolution TEM.

Methods

In an in-situ XRD experiment, the precursor $\text{Co}(\text{OH})_2$ underwent calcination to 1200°C in steps of 25°C in synthetic air (20% O_2), mapping the crystal-size evolution of Co_3O_4 and its phase transitions. For visualization of the sample morphologies by electron microscopy, several Co_3O_4 samples were prepared separately by calcining $\text{Co}(\text{OH})_2$ at varying temperatures. The choice of temperatures was based on the in-situ XRD experiment.

Transmission electron microscopy was carried out using a probe-corrected Spectra 200 (S)TEM (Thermo Fischer Scientific), operated at 200 kV in scanning mode (STEM), or in parallel beam mode (TEM) for high-resolution imaging. Electron tomography tilt series were acquired in scanning mode using the high-angle annular dark field detector (STEM-HAADF) and a low convergence angle of 5.6 mrad for enhanced depth-of-field [5]. The tilt-series, recorded from $+70$ to -70 degrees in 2-degree intervals, were reconstructed into a tomogram with voxel size $(0.43 \text{ nm})^3$ using fiducial marker tracking (10nm) and weighted back projection (WBP) in Inspect3D v.4.5. The crystallographic orientation of the reconstruction was determined from additional high-resolution TEM images. Finally, the facet distribution of the 3D reconstructed Co_3O_4 particle was evaluated from a 3D printed model of the reconstructed volume, by identifying the facets.

Results

The decomposition of $\text{Co}(\text{OH})_2$ in synthetic air to form Co_3O_4 initiated at 150°C . As the calcination process continued, the mean crystal size of Co_3O_4 , as measured by XRD, gradually

increased from about 10 nm to 500 nm, indicating sintering. The maximum sintering rate was observed around 850°C, right before an abrupt full phase transition into CoO, which occurred between 875°C and 900°C. Upon cooling, the CoO phase fully transformed back to a Co₃O₄ structure with an average crystallite size (XRD) of ~150 nm. (S)TEM images confirm the presence of both large and small Co₃O₄ nanocrystals in the residual sample.

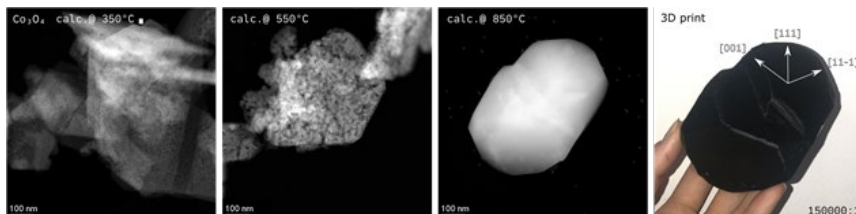
STEM imaging reveals that the cobalt spinel samples, calcined at 350°C, 450°C, and 550°C, are present in a pseudo-morph structure, resembling the overall shape of the hydroxide precursor, across all three samples. This morphology can be characterized as monocrystalline mesoporous nanograin sheets. While the sheet morphology is consistent across all three samples, an increase in the size of both the grains and pores is observed with increasing calcination temperature.

STEM images of a sample calcined at a high sintering rate (850°C), revealed large particles which appear to be partly faceted. One particle was reconstructed in 3D, revealing clear facets with the (100) facet being predominantly present, followed by (111) and (110). 24% of the surface could not be identified due to rounding, suggesting that the facet formation was not fully completed or equilibrated. This observation was supported by a 50-hour XRD experiment which showed that the mean crystal size of Co₃O₄ initially converges after several hours at 850°C, revealing that the 1-hour heated sample was captured in a dynamic sintering process.

Conclusion

By utilizing electron microscopy – specifically tomography – we were able to observe the morphological changes of Co₃O₄ synthesized by calcination of Co(OH)₂ at various temperatures. The Co₃O₄ samples exhibited a sheet-like monocrystalline mesoporous nanograin structure at 350°C and underwent drastic morphological changes as the material sintered to form large particles at higher temperatures. The shape and facet distribution of a Co₃O₄ crystal (calcined at 850°C for 1 hour) were determined using electron tomography combined with high-resolution TEM imaging, revealing the (100) facet as predominantly present, followed by (111) and (110). This approach provides valuable insights into the complex transformation processes (e.g., sintering) occurring in catalytic processes.

Graphic:



Keywords:

Co₃O₄, morphology, sintering, facet distribution

Reference:

- Sun, T. et al. Chem. Eng. J. 390, 124591 (2020)
Ma, H. et al. ACS Appl. Mater. Interfaces 8 (2016)
Seo, J.H. et al. J Anal Sci Technol 14, 31 (2023).
Li, M. et al. Catal. Today 376, 177 (2021)
Bals, S. et al. Angew Chem Int Ed 53, 10600 (2014)